IEEE Access
Multidisciplinary | Rapid Review | Open Access Journal

Received February 13, 2019, accepted March 7, 2019, date of publication March 26, 2019, date of current version April 9, 2019.

Digital Object Identifier 10.1109/ACCESS.2019.2906861

Backstepping and Robust Control for a Quadrotor in Outdoors Environments: An Experimental Approach

ORLANDO GARCÍA[1], PATRICIO ORDAZ[2], OMAR-JACOBO SANTOS-SÁNCHEZ[2], SERGIO SALAZAR[1], AND ROGELIO LOZANO[1], (Member, IEEE)

[1]UMI-LAFMIA, Center for Research and Advanced Studies (CINVESTAV), Mexico City 07360, Mexico
[2]Electronic and Control Academic Group, Research Center on Technology of Information and Systems (CITIS), Autonomous University of Hidalgo State (UAEH), Pachuca de Soto 42184, Mexico

Corresponding author: Omar-Jacobo Santos-Sánchez (omarj@uaeh.edu.mx)

This work was supported by PRODEP-Mexico.

ABSTRACT This paper addresses the tracking control of quadrotors flying outdoors. Two control laws are combined and tested in real-time experiments. The aircraft attitude and the translational displacement are controlled using the backstepping approach, while the altitude is controlled using the sliding mode control strategy. In both cases, new modifications are introduced with respect to the existing classical algorithms. Concerning the backstepping algorithm, we introduce the dynamical model of the quadrotor in the controller design and this guarantees that the virtual input is bounded. On the other hand, the proposed sliding mode control assures that the vehicle's altitude converges in finite time to the desired reference, even when uncertainties are considered in the system. The proposed controller is tested in an outdoor environment and the experiments highlighted the controllers' reliability. Additionally, the performance of the closed-loop plant with the proposed controllers is compared with the performance given by a proportional-derivative controller.

INDEX TERMS Backstepping control, sliding mode control, nonlinear systems, quadrotor.

I. INTRODUCTION

The trajectory tracking task for quadrotors evolving in outdoors environments is a very common mission [2]. However, the nonlinear nature of these type of aircrafts makes it difficult to guarantee the stability of the closed loop control system. Some common techniques used in nonlinear systems, in particular in UAVs, are the Backstepping (BS) algorithm and the Sliding Mode Control (SMC). The former guarantees stability while the latter provides robustness with respect to external disturbances, parameters and/or dynamic uncertainties. In the last decade, several control algorithms have been proposed for unmanned vehicles stabilization, for instance, in [1] a vision-based stabilization and output tracking control method for a model helicopter was proposed. Furthermore, two methods of control were studied: one using a series of model-based, feedback linearizing controllers and the other using a BS-like control law, simulation and experimental results for indoors environment were presented. [3] presents a quadrotor controller for the tracking of a moving ground target. Moreover, to eliminate the need for inverse kinematics in a full state BS control architecture, the BS method was used via a re-formulated full state cascaded dynamics. The problem of designing and experimentally validating a controller for steering a quadrotor vehicle along a trajectory, while rejecting constant force disturbances, was addressed in [4]. The proposed solution consists of a linear adaptive state feedback controller that asymptotically stabilizes the closed-loop system in the presence of force disturbances. Experimental results were presented. In [5], a nonlinear controller for a quadrotor helicopter, which guarantees the global asymptotic stabilization was proposed. The controller was synthesized by Command Filtered BS method. Experimental flight tests were presented. In [16], a BS-based nonlinear controller was developed to control the quadrotor in the presence of constant and time-varying disturbances. Simulation results were presented.

SMC approaches attract a lot attention in UAV for trajectory tracking and hover flight because of their robustness properties [6]–[10]. The SMC main advantage is the finite

The associate editor coordinating the review of this manuscript and approving it for publication was Giovanni Angiulli.

time convergence to the sliding manifold [11]. Therefore, the SMC controller can reject external disturbances. In [8], a comparative study between Feedback Linearization an adaptive SMC using augmented input to control a quadrotor was addressed. Experimental tests of a combination of BS and SMC for quadrotor control are presented in [12]. The concept of partial trajectory collapse in SMC has been addressed in [6], [11], [14] where the sliding manifold is designed in order to collapse in finite time. This fact is achieved using a fractional power in the sliding surface [11], [14], [15]. A finite-time hover stabilization was proposed in [13], via a terminal SMC. Most papers in the literature deal with modifications to classical algorithms to improve the performance when disturbances occur. However such robustness could sometime be obtained at the Price of spending more energy [18] and consequently the flight time is reduced [19]. The simplicity of the classical algorithm was highlighted in [1] for hover flight. However the experimental validation was carried out indoor only.

In [25], two control techniques were applied to the flight problem in the formation of UAVs, one based on a PID and the other a control by integral sliding modes to reject time-varying disturbances. Experimental results were obtained using the Vicon vision system. The control signals were calculated in a ground station. Another similar work is [28] where a comparison between three algorithms is made: the classic PID controller, a BS control and a SMC. Simulation results were presented for the control of the attitude of a four-rotor aircraft.

In the present paper we retain the simplicity of the original BS algorithm to control a quadrotor via a simple transformation. As will be seen later, the proposed transformation is different from the one used in [1]. We use the fact that the quadrotor model involves a sinusoidal function for the subsystems '$y - \varphi$' and '$x - \theta$'. This transcendental function guarantees that the virtual input is always bounded, and consequently the obtained control input could be smoother than the input issued from a robust controller. Furthermore, the proposed control law is experimentally validated for trajectory tracking in outdoors flight. Another objective of this work is to control the aerial vehicle without separating the rotational and the translational dynamic models. Such a task can be carried out by the proposed controller based on the BS algorithm. Most of the previous papers on the BS control deal separately with the rotational part of the translational part. The main contribution of the paper is the implementation of the BS control to the whole quadcopter dynamics. The BS approach is combined with SMC for the altitude control, to guarantee that the altitude reaches a value arbitrarily close to the desired value in finite time [11], It allows a better control in the x and y axis. The SMC presented in this paper is a new control strategy and, to the best of our knowledge, it has not been previously reported in the literature. Furthermore, the singularity in the traditional Terminal SMC when the trajectory arrives to the sliding surface is avoided, which represents also a contribution of this paper.

The paper highlights are the following:

- The Backstteping (BS) algorithm was modified to consider a bounded virtual input: a sinusoidal function. The boundedness of the virtual input guarantees the smooth of the control law.
- The SMC designed here, allows the finite time convergence, avoiding singularities on the control law.
- The structure of the proposed SMC control law can be further simplified. Moreover, a simplified translational control law can be obtained when the modified BS are calculated.
- In contrast to previous reported results, both proposed control algorithms were join to improve the performance of the quadrotor vehicle, and satisfactory tests (according with the hardware limitations) in outdoor environment were carried out.
- The proposed join control algorithm effectiveness is demonstrated through successfully outdoor tests.

The article is organized as follows: Preliminaries results are presented in Section II. Section III describes the controller synthesis for the quadrotor, the description of the experimental platform and the implementation of proposed controllers. Finally the concluding remarks are given in Section IV.

II. BACKSTEPPING AND SLIDING MODE CONTROLLERS DESIGN

This section presents the quadrotor controller synthesis. In order to guarantee convergence of the altitude (z and $\dot{z}$) to its desired value in finite time subject to external bounded disturbances and unmodeled dynamics, we propose an SMC controller. Such a controller should improve the performance of the aircraft behavior in closed loop.

A. MODIFIED BACKSTEPPING ALGORITHM USING A SINE FUNCTION AS VIRTUAL INPUT

In this section, the modified Backstepping method is developed when the virtual input is the function $\sin(\zeta)$, where $\zeta \in (-\frac{\pi}{2}, \frac{\pi}{2})$, this domain guarantees that the only solution for $\sin(\zeta) = 0$ is zero. Such a constraint is sufficient to deal with the case of the quadrotor. Notice that in the classical algorithm, the virtual input is only ζ [20], [21]. Consider the following system:

$$\begin{aligned} \dot{\eta}(t) &= f(\eta(t)) + g(\eta(t))\sin(\zeta(t)), \\ \dot{\zeta}(t) &= u, \end{aligned} \tag{1}$$

where $\eta \in \Re^n$, $\zeta \in \Re$, $u \in \Re$, . In this paper, we assume the following:

1) The functions $f : D \subseteq \Re^n \longrightarrow \Re^n$ and $g : D \subseteq \Re^n \longrightarrow \Re^n$ are continuously differentiable,
2) $f(0) = 0$ and $\eta = 0 \in D$,
3) $\zeta \in (-\frac{\pi}{2}, \frac{\pi}{2})$.

The classical problem is how to find an input u such that $\eta = 0$ and $\zeta = 0$ are asymptotically stable, however for the structure given by the equation (1), the function $\sin(\cdot)$ guarantees that this virtual input is always bounded. The control

strategy proposed in [1] used a different transformation of state variables. In the present paper we use a modified BS algorithm in an iterative way. Since the system structure is given by (1) then the virtual input for the equations of translational position and velocity are bounded. Now, consider the following Proposition:

Proposition 1 (Modified BS Control Algorithm): Let the system given by equation (1)*, under the assumptions described above, a control u which locally stabilizes to the system* (1) *is given as follows:*

$$u = \frac{\frac{\partial \varphi}{\partial \eta}\left[f(\eta)+g(\eta)\sin(\zeta)\right] - k\left(\sin(\zeta)\text{-}\varphi(\eta)\right) - \frac{\partial V(\eta)}{\partial \eta}g(\eta)}{\cos(\zeta)}. \tag{2}$$

where $k > 0$, $\varphi(\eta)$ and $V(\eta) > 0$ are known functions.

Proof: The proof is based on the classical Backstepping algorithm [21] and assumes that there exists a function $\varphi(\eta)$ such that $\varphi(0) = 0$ and the system:

$$\dot{\eta} = f(\eta) + g(\eta)\varphi(\eta), \tag{3}$$

has a stable trivial solution. Then, assume that there exists a smooth and positive definite function $V(\eta)$ which satisfies:

$$\left.\frac{dV(\eta)}{dt}\right|_{(3)} = \frac{\partial V}{\partial \eta}\left[f(\eta) + g(\eta)\varphi(\eta)\right] \leq -W(\eta), \quad \forall \eta \in D,$$

where $W(\eta)$ is a known positive definite function. Thus, the state space equation (1) is rewritten as:

$$\begin{aligned} \dot{\eta} &= f(\eta) + g(\eta)\varphi(\eta) + g(\eta)[\sin(\zeta) - \varphi(\eta)], \\ \dot{\zeta} &= u. \end{aligned} \tag{4}$$

Let $\varkappa$ be a deviation variable $\varkappa \triangleq \sin(\zeta) - \varphi(\eta)$ and its derivative can be calculated as $\dot{\varkappa} = \cos(\zeta)\dot{\zeta} - \dot{\varphi} = \cos(\zeta)\, u - \dot{\varphi}$. Then, system (4) can be expressed as a function of the $\varkappa$ variable:

$$\begin{aligned} \dot{\eta} &= \overbrace{f(\eta) + g(\eta)\varphi(\eta)}^{\bar{f}(.)} + g(\eta)\varkappa, \\ \dot{\varkappa} &= \cos(\zeta)u - \dot{\varphi}, \end{aligned} \tag{5}$$

as the classical BS algorithm when $\varkappa = 0$, it is possible to guarantee that (5) has a stable equilibrium at the origin, and the time derivative of φ is:

$$\dot{\varphi}(\eta) = \frac{\partial \varphi}{\partial \eta}\dot{\eta} = \frac{\partial \varphi(\eta)}{\partial \eta}\left[f(\eta) + g(\eta)\sin(\zeta)\right].$$

Now, define $\nu \triangleq \cos(\zeta)u - \dot{\varphi}$, with this expression the system can be represented as follows:

$$\begin{aligned} \dot{\eta} &= \bar{f}(\eta) + g(\eta)\varkappa, \\ \dot{\varkappa} &= \nu. \end{aligned} \tag{6}$$

On the other hand, consider the following positive definite function:

$$V_a(\eta, \varkappa) = V(\eta) + \frac{1}{2}\varkappa^2,$$

notice that, $V_a(\cdot)$ could be a candidate Lyapunov function for the system (6), then the time derivative of this function is:

$$\begin{aligned} \left.\frac{dV_a(\eta, \varkappa)}{dt}\right|_{(6)} &= \frac{\partial V(\eta)}{\partial \eta}\bar{f}(\eta) + \frac{\partial V(\eta)}{\partial \eta}g(\eta)\varkappa + \varkappa\nu \\ &\leq -W(\eta) + \frac{\partial V(\eta)}{\partial \eta}g(\eta)\varkappa + \varkappa\nu. \end{aligned}$$

By selecting: $\nu \triangleq -k\varkappa - \frac{\partial V(\eta)}{\partial \eta}g(\eta)$, where $k > 0$, and substituting in the previous equation, we get:

$$\left.\dot{V}_a(\eta, \varkappa)\right|_{(6)} \leq -W(\eta) - k\varkappa^2 < 0, \tag{7}$$

so, the system given by (6) has an asymptotically stable trivial solution ($\eta = 0$ and $\varkappa = 0$). The input u can be obtained from (5) as follows

$$\begin{aligned} u &= \frac{\dot{\varkappa} + \dot{\varphi}}{\cos(\zeta)} = \frac{\nu + \dot{\varphi}}{\cos(\zeta)} \\ &= \frac{-k\left(\sin(\zeta) - \varphi(\eta)\right) - \frac{\partial V(\eta)}{\partial \eta}g(\eta) + \frac{\partial \varphi}{\partial \eta}\left[f(\eta) + g(\eta)\sin(\zeta)\right]}{\cos(\zeta)}, \\ &\quad \cos(\zeta) \neq 0. \end{aligned}$$

and this concludes the proof. □

The above control law based on the modified BS algorithm stabilizes system (1). It can be applied outdoors to control the quadrotor flight. The SMC control synthesis is presented in the next section and the experimental tests are afterward.

B. PARTIAL TRAJECTORY COLLAPSE VIA TERMINAL SMC WITHOUT SINGULARITIES

Consider the following nonlinear system:

$$\begin{aligned} \dot{\xi}_1 &= \xi_2, \, \|f(\xi, t)\| \leq \delta_1 < \infty, \\ \dot{\xi}_2 &= f(\xi, t) + \bar{g}(\xi)u, \, \xi(0) = \xi_0, \quad \text{a. e. } t \in \Re^+, \end{aligned} \tag{8}$$

where $\xi = [\xi_1, \xi_2]^T$ is the state space, $f : \Re \to \Re$ is a nonlinear function which includes uncertain dynamics and/or external disturbances, $u \in \Re$ is the control input and its realizing function is denoted by $\bar{g}(\xi) \in \Re$. The aim of this section is to guarantee that the trajectory convergence $\xi_1 = 0$ and $\xi_2 = 0$ be reached in finite time. This control objective can be achieved by using SMC, see for instance [11], section 2.8. To this end, the sliding manifold is established, in such a way, that the ξ_1 converges to zero in finite time. From (8), notice that $\dot{\xi}_1 = \xi_2$, thus, if the trajectory ξ_1 converges to zero in finite time, the error ξ_2 converges too. Next proposition establishes the sliding surface which will guarantee the finite time convergence.

Proposition 2 (Finite Time Convergence): Consider the sliding manifold

$$S = \xi_2 + R\xi_1|\xi_1|^{-\frac{1}{3}}, \; 0 < R \in \Re, \tag{9}$$

if $S = 0$ for all $t \geq t_r$, then, from the trajectory $\xi = 0$ in time

$$T = \frac{3}{R}|\xi_1(0)|^{\frac{1}{3}} + t_r. \tag{10}$$

Proof: Under the assumption that $\dot{\xi}_1 = \xi_2$, where $S = 0$ is fulfilled, then

$$\dot{\xi}_1 = -R\xi_1|\xi_1|^{-\frac{1}{3}},\ \xi_1(0) = \xi_1^0,$$

therefore the next ordinary differential equation with discontinuous right hand side is obtained

$$-Rdt = \frac{|\xi_1|^{\frac{1}{3}}d\xi_2}{\xi_1},$$

integrating over the integration variable $\tau \in [t_r, t)$

$$-R\int_{t_r}^{t} d\tau = \int_{t_r}^{t} \frac{|\xi_1|^{\frac{1}{3}}d\xi_2}{\xi_1}.$$

The solution of the previous equation gives

$$\xi_1(t) = \pm\left|\left(|\xi_1(t_r)|^{\frac{1}{3}} - \frac{R}{3}(t - t_r)\right)^3\right|,$$

by substituting $t = T$, where T is given by equation (10), it follows the trajectory $\xi_1(t)$ converges to zero in finite time, and the Proposition is proven. □

Once the sliding manifold is fixed, the control function design which guarantees the finite time convergence of sliding manifold, is presented in the next proposition.

Proposition 3 (On the Sliding Control Function): If the control action for the system (8) *is defined as*

$$u = \begin{cases} -\dfrac{1}{\bar{g}(\xi)}\left\{\dfrac{2}{3}R\xi_2|\xi_1|^{-\frac{1}{3}} + \rho Sign(S)\right\}, & \xi_1 \neq 0 \\ -\dfrac{1}{\bar{g}(\xi)}\rho Sign(S), & \xi_1 = 0 \end{cases} \tag{11}$$

then, the sliding manifold S converges to zero in the following finite time

$$t_r = \frac{\sqrt{2}}{\alpha_2}V_1^{\frac{1}{2}}(S(t_0)) + t_0, \tag{12}$$

where $\alpha_2 = \rho_2 - \delta_2 > 0$.

Proof: Consider next quadratic storage function

$$V(S) = \frac{1}{2}S^2.$$

Its time variations along the trajectories to the system (8), fulfills next relation

$$\dot{V}(S)\big|_{(8)} = S\left\{\dot{\xi}_2 + R\dot{\xi}_1|\xi_1|^{-\frac{1}{3}} + R\xi_1\left(-\frac{1}{3}|\xi_1|^{-\frac{4}{3}}\frac{d}{dt}|\xi_1|\right)\right\}. \tag{13}$$

Notice that, the time derivative of $|\xi_1|$ yields

$$\begin{aligned}\frac{d}{dt}|\xi_1| &= \frac{d}{dt}(\xi_1^2)^{\frac{1}{2}} = \frac{1}{2}(\xi_1^2)^{-\frac{1}{2}}\frac{d}{dt}\xi_1^2 = (\xi_1^2)^{-\frac{1}{2}}\xi_1\frac{d}{dt}\xi_1 \\ &= (\xi_1^2)^{-\frac{1}{2}}\xi_1\dot{\xi}_1 = \frac{\xi_1}{|\xi_1|}\dot{\xi}_1 = \mathrm{Sign}(\xi_1)\dot{\xi}_1.\end{aligned}$$

Thus, the derivative (13), is given by

$$\frac{d}{dt}V(S)\bigg|_{(8)} = S\left\{f(\xi,t) + \bar{g}(\xi)u + \frac{2}{3}R\xi_2|\xi_1|^{-\frac{1}{3}}\right\},$$

by using the control function given by (11), then

$$\begin{aligned}\frac{d}{dt}V(S) = S\Bigg\{f(\xi,t) - \left(\frac{2}{3}R\xi_2|\xi_1|^{-\frac{1}{3}} + \rho\mathrm{Sign}(S)\right) \\ + \frac{2}{3}R\xi_2|\xi_1|^{-\frac{1}{3}}\Bigg\} = S\left\{f(\xi,t) - \rho\mathrm{Sign}(S)\right\}.\end{aligned}$$

Since $\|f(\xi,t)\| \leq \delta_1$, at least from the local point of view, if $\rho > \delta_1$, previous equation yields

$$\begin{aligned}\frac{d}{dt}V(S) &= Sf(\xi,t) - S\rho\mathrm{Sign}(S) = -\rho|S| + Sf(\xi,t) \\ &\leq -\rho|S| + |S||f(\xi,t)| \leq -\rho|S| + |S|\delta \\ &\leq -(\rho - \delta)|S| \leq -\alpha|S|,\end{aligned}$$

then

$$\dot{V}_1(S) \leq -\alpha_2|S| = -\alpha_2\sqrt{2}\,V_1^{\frac{1}{2}}(S), \tag{14}$$

and previous differential inequality fulfills next solution

$$V_1^{\frac{1}{2}}(S(t)) \leq V_1^{\frac{1}{2}}(S(t_0)) - \frac{\alpha_2}{\sqrt{2}}(t - t_0),$$

which means that the sliding variable converges to the origin in the finite time (12). After this specific time, the sliding motion $S = 0$ for all $t \geq t_r$, which means that $\dot{\xi}_1 = -R\xi_1|\xi_1|^{-\frac{1}{3}}$, and the control action takes place as

$$\begin{aligned}u &= -\frac{1}{\bar{g}(\xi)}\left\{\frac{2}{3}R\xi_2|\xi_1|^{-\frac{1}{3}} + \rho\mathrm{Sign}(S)\right\} \\ &= -\frac{1}{\bar{g}(\xi)}\left\{-\frac{2}{3}R^2\xi_1|\xi_1|^{-\frac{2}{3}} + \rho\mathrm{Sign}(S)\right\}\end{aligned}$$

however, $\xi_1 = |\xi_1|\mathrm{Sign}(\xi_1)$, thus

$$\begin{aligned}u &= -\frac{1}{\bar{g}(\xi)}\left\{-\frac{2}{3}R^2\frac{|\xi_1|\mathrm{Sign}(\xi_1)}{|\xi_1|^{-\frac{2}{3}}} + \rho\mathrm{Sign}(S)\right\} \\ &= -\frac{1}{\bar{g}(\xi)}\left\{-\frac{2}{3}R^2\mathrm{Sign}(\xi_1)|\xi_1|^{\frac{1}{3}} + \rho\mathrm{Sign}(S)\right\}\end{aligned}$$

and this is a non singular control action. Furthermore, for the case when $\xi_2 = 0$, it is evident that $S > 0$ and $S < 0$ implies that $-\alpha \leq \dot{\xi}_2 \geq \alpha$, this means that in general $\xi_2 = 0$ is not an attractor. However, for the case where $\xi_1 = 0$ and $\xi_2 \neq 0$, the sliding surface takes place as $S = \xi_2$, so the time derivative of its storage function has next format

$$\frac{d}{dt}V(S)\bigg|_{(8)} = S\left\{f(\xi,t) + \bar{g}(\xi)u\right\},$$

and the controller which satisfies (14) is given by

$$u = -\frac{\rho\mathrm{Sign}(S)}{\bar{g}(\xi)}$$

showing that $\xi_2 = 0$ is an attractor when $\xi_1 = 0$, which completes the proof. □

Previous Proposition established that the sliding variable (9) converges to zero in finite time. Thus, Filippov's concept for differential equations with discontinuous right-hand sides implies that the sliding variable S remains around the origin for all future time $t \geq t_r$. This means that, Proposition 2

is fulfilled too, thus, the trajectory $\xi_1 \to 0$ when $t \to T$, remains equal to zero for all future time. Finally if $\xi_1 = 0$ for all $t \geq T$, then its time variations are zero, which implies that $\dot{\xi}_1 = \xi_2 = 0$.

III. QUADCOPTER MODEL

The quadcopter is an aerial vehicle that consists of 4 rotors, the mathematical model can be divided into two parts, the translational part and the rotational part. In order to make the control synthesis, the following equations were used that describe the movement of a rigid body [27] which are based on the Euler-Lagrange formalism:

$$\begin{aligned} m\ddot{z} &= ucos\theta \cos\varphi \\ m\ddot{x} &= -u\sin\theta \\ m\ddot{y} &= ucos\theta \sin\varphi \end{aligned} \tag{15}$$

$$\begin{aligned} \ddot{\theta} &= \dot{\phi}\dot{\psi}\left(\frac{I_x - I_z}{I_y}\right) + \frac{l}{I_y}\tau_\theta \\ \ddot{\varphi} &= \dot{\theta}\dot{\psi}\left(\frac{I_y - I_z}{I_x}\right) + \frac{l}{I_x}\tau_\varphi \\ \ddot{\psi} &= \dot{\varphi}\dot{\theta}\left(\frac{I_y - I_x}{I_z}\right) + \frac{l}{I_z}\tau_\psi \end{aligned} \tag{16}$$

where (x, y, z) are the Cartesian Coordinates ie. the relative position of the mass center of the quadcopter with respect to an inertial frame, (φ, θ, ψ) represent the attitude of the vehicle, these angles are known as (roll, pitch and yaw) and τ_φ τ_θ, τ_ψ are the torques that allow the movement of roll, pitch and yaw respectively. m is the mass of the vehicle, l is the arm length. I_x, I_y, I_z are the moments of inertia in 3 axes.
This model can be divided into subsystems which will be described later.
For this type of vehicle the following assumptions are considered:

- The quadcopter has a rigid and symmetrical structure.
- The center of gravity of the vehicle coincides with the origin of the body frame.
- The propellers are rigid with fixed pitch.
- At low speeds, aerodynamic effects can be neglected.
- The rotor dynamics is approximately equal to one, because the time constant in the first-order transfer function is small (See [26]).
- The angles ϕ, θ and ψ are bounded between $-\pi/4$ and $\pi/4$.

IV. IMPLEMENTATION AND EXPERIMENTAL RESULTS

A trajectory tracking task in outdoors environment for a quadrotor is a crucial mission in this type of unmanned vehicles. Actually, this class of systems is exposed to external disturbances that may provoke instability. In this sense, an important issue for the control technology of these systems, deals with robust controllers design which guarantees a suitable performance. In order to improve the performance of quadrotor outdoors, in this section the controllers designed in previous section and its real-time application is presented. To this end, the system is divided into four subsystems. First, the altitude subsystem is controlled by the SMC, see Proposition 3. The other subsystems, yaw ψ, $x-\theta$ and $y-\varphi$ subsystems, are controlled by the modified-BS algorithm, see Proposition 1.

A. SLIDING MODE CONTROL APPLIED TO THE DYNAMICS OF z

The simplified mathematical model for a quadrotor could be found in the specialized literature, for example see [19]. In that work, the equations are split into subsystems: altitude subsystem represented by z, the yaw subsystem called ψ, the translational and roll subsystem denoted by $x - \theta$ and translational and pitch subsystem defined $y-\varphi$, [19]. In order to maintain the quadrotor altitude close to its desired value, under uncertainty dynamics and/or external bounded disturbances, in this subsection the partial trajectory collapse for quadrotor altitude via Terminal SMC is presented. Just notice that, the dynamics of subsystem z is described as follows [19]:

$$m\ddot{z} = u\cos(\theta)\cos(\varphi) - mg.$$

To apply the terminal SMC proposed in this paper, consider the next change of variables: $\xi_1 = z$, $\xi_2 = \dot{z}$, thus, the above equation can be written as

$$\begin{aligned} \dot{\xi}_1 &= \xi_2, \\ \dot{\xi}_2 &= \frac{u}{m}\cos(\theta)\cos(\varphi) - g + \delta(t), \end{aligned} \tag{17}$$

where the parameter m and g are the vehicle mass and the gravity constant, respectively. For this system, notice that $f(\xi, t) = -g + \delta(t)$, and $|\delta(t)| \leq \delta_0$ so, $\delta_1 = g + \delta_0$, where $\delta(t)$ represents the external bounded disturbances. Furthermore, $\bar{g}(\xi) = \frac{1}{m}\cos(\theta)\cos(\varphi)$ is bounded. In this way, from Proposition 3, the attitude flight control for (17) is characterized by

$$u = \begin{cases} \bar{u}, & \xi_1 \neq 0 \\ -\frac{1}{\bar{g}(\xi)}\rho\text{Sign}(\xi_2), & \xi_1 = 0 \end{cases}$$

$$\bar{u} = -\frac{1}{\bar{g}(\xi)}\left\{\frac{2}{3}R\xi_2|\xi_1|^{-\frac{1}{3}} + \rho\text{Sign}\left(\xi_2 + R\xi_1|\xi_1|^{-\frac{1}{3}}\right)\right\} \tag{18}$$

and under assumption that, for hover flight $\theta \approx 0$ and $\varphi \approx 0$, the control law is approximated as

$$u = \begin{cases} -\frac{2}{3}R\xi_2|\xi_1|^{-\frac{1}{3}} - \rho\text{Sign}(\xi_2 + R\xi_1|\xi_1|^{-\frac{1}{3}}), & \xi_1 \neq 0, \\ -\rho\text{Sign}(\xi_2), & \xi_1 = 0, \end{cases}$$

which means that before time

$$T = \frac{3}{R}|\xi_1(0)|^{\frac{1}{3}} + \frac{1}{\alpha_2}|S(\xi_2(0) + R\xi_1(0)|\xi_1(0)|^{-\frac{1}{3}})| + t_0,$$

attitude system converges in the finite time T to the Set Point. Notice that, for this class of systems, the SMC applied in altitude regulation is not directly applied on the actuator, i.e. the altitude control is given from a forces combination given by each rotor. Moreover, the control signal (18), is computed in the Pixhawk autopilot and it is traduced to voltage input for each motor by using power interface based on PWM. In this way, the chattering effect given by SMC is attenuated by the hardware of the plant.

B. SUBSYSTEM ψ

The second subsystem to be controlled describes the yaw angle dynamics [19], and it is represented as:

$$\ddot{\psi} = \dot{\varphi}\dot{\theta}k_1 + g_1\tau_\psi,$$

where $k_1 = \frac{(\mathbb{I}_y - \mathbb{I}_x)}{\mathbb{I}_z}$, $g_1 = \frac{l}{\mathbb{I}_z}$ and $\mathbb{I}_x$, $\mathbb{I}_y$, $\mathbb{I}_z$ are the Inertia Matrix parameters. While the following change of variable $x_3 = \psi$, $x_4 = \dot{\psi}$ is considered, under pre-compensation $\tau_\psi = \frac{1}{g_1}(-\dot{\varphi}\dot{\theta}k_1 + u_{a\psi})$, previous subsystem is rewritten as a double integrator system as:

$$\begin{aligned}\dot{x}_3 &= x_4\\ \dot{x}_4 &= u_{a\psi}.\end{aligned}$$

Now, by selecting $x_4 = \varphi(x_3) = -\alpha_\psi x_3$, as is described in (1), the above double integrator systems can be rewritten as

$$\begin{aligned}\dot{x}_3 &= -\alpha_\psi x_3\\ \dot{x}_4 &= u_{a\psi}.\end{aligned}$$

Thus, according to Proposition 1, an associate Lyapunov function can be defined as:

$$V_\psi(x_3) = \frac{1}{2}x_3^2,$$

and the control input $u_{a\psi}$ has the following structure:

$$u_{a\psi} = -k_\psi \varkappa - \frac{\partial V_\psi(\eta)}{\partial \eta}g(\eta) + \frac{\partial(\varphi)}{\partial \eta}\left[f(\eta) + g(\eta)\zeta\right]. \quad (19)$$

by assuming that, $\varkappa = x_4 + \alpha_\psi x_3$, $\zeta = x_4$, $\eta = x_3$, $f(\eta) = 0$, $g(\eta) = 1$, the control law which stabilizes the yaw subsystem is given by:

$$u_{a\psi} = -\alpha_\psi x_4 - x_3 - k_\psi\left(x_4 + \alpha_\psi x_3\right).$$

C. SUBSYSTEM $x - \theta$

Let the subsystem which describes the translational movement in the x axis and the pitch angle [19]. Notice that the subsystem $x - \theta$ is described as follows:

$$\begin{aligned}\ddot{x} &= -\frac{1}{m}\sin(\theta)u\\ \ddot{\theta} &= \dot{\varphi}\dot{\psi}k_2 + g_2\tau_\theta,\end{aligned}$$

where $k_2 = \frac{(\mathbb{I}_x - \mathbb{I}_z)}{\mathbb{I}_y}$ and $g_2 = \frac{l}{\mathbb{I}_y}$, where $\mathbb{I}_x, \mathbb{I}_z$ and $\mathbb{I}_y$ are the inertia moments in the respective frame. Notice that u does not depend on variables $x, \dot{x}, \theta, \dot{\theta}$, so, the control action u in the subsystem $x - \theta$, is only a bounded time function, and as it is established in the previous section, it converges to a fixed value in finite time. Now, consider the following variable changes: $x_5 = x$, $x_6 = \dot{x}$, $x_7 = \theta$, $x_8 = \dot{\theta}$, where its state space representation is:

$$\begin{aligned}\dot{x}_5 &= x_6\\ \dot{x}_6 &= -\frac{1}{m}\sin(x_7)u(t)\\ \dot{x}_7 &= x_8\\ \dot{x}_8 &= \dot{\varphi}\dot{\psi}k_2 + g_2\tau_\theta,\end{aligned}$$

where, $|u(t)| \leq \delta_2$, $\delta_2 < \infty$. Taking the first and the second equation from the state space representation and choosing a virtual input u_{1x}:

$$u_{1x} = \sin(x_7) = -\frac{m}{u(t)}u_{ax} \quad (20)$$

where u_{ax} is the control input. Now, it follows that:

$$\begin{aligned}\dot{x}_5 &= x_6\\ \dot{x}_6 &= u_{ax}.\end{aligned}$$

According to the BS control algorithm, $x_6 = \varphi(x_5) = -\alpha_{1x}x_5$, where $\alpha_{1x} > 0$ and we obtain:

$$\begin{aligned}\dot{x}_5 &= \alpha_{1x}x_5\\ \dot{x}_6 &= u_{ax}.\end{aligned}$$

For the last subsystem, an associate Lyapunov function is proposed as:

$$V_{1x}(x_5) = \frac{1}{2}x_5^2, \quad (21)$$

so, according to BS algorithm control, the input u_{ax} can be computed as:

$$u_{ax} = \left(-x_5 - \alpha_{1x}x_6 - k_{1x}(x_6 + \alpha_{1x}x_5)\right),$$

and substituting the control u_{ax} into (20), it follows that:

$$u_{1x} = -\frac{m}{u(\cdot)}\left(-x_5 - \alpha_{1x}x_6 - k_{1x}(x_6 + \alpha_{1x}x_5)\right).$$

Applying the iterative BS control algorithm, the following representation is obtained:

$$\begin{aligned}\dot{x}_5 &= x_6\\ \dot{x}_6 &= -\frac{1}{m}\sin(x_7)u(t)\\ \dot{x}_7 &= x_8.\end{aligned} \quad (22)$$

By using Proposition 1, next statement follows:

$$\begin{aligned}\begin{bmatrix}\dot{x}_5\\ \dot{x}_6\end{bmatrix} &= \begin{bmatrix}x_6\\ 0\end{bmatrix} + \begin{bmatrix}0\\ -\frac{u(\cdot)}{m}\end{bmatrix}\sin(\zeta_0)\\ \dot{\zeta}_0 &= x_8 = u_{2x},\end{aligned}$$

where $\zeta_0 = x_7$. Following the iterative BS algorithm, a new Lyapunov function is proposed:

$$V_{2x}(x_5, x_6) = \frac{1}{2}x_5^2 + \frac{\alpha_{2x}}{2}\left(x_6 + \alpha_{1x}x_5\right)^2, \quad (23)$$

where α_{2x} is a proposed parameter to set the convergence speed. The virtual input $\varphi_{1x} = \sin(\zeta_0)$ and according to the iterative BS algorithm, it is defined by the previous virtual input u_{1x}, then:

$$\varphi_{1x}(x_5, x_6) = -\frac{m}{u(\cdot)}(-x_5 - \alpha_{1x}x_6 - k_{1x}(x_6 + \alpha_{1x}x_5)),$$

then, following Proposition 1, the partial derivatives of φ_{1x} and V_{2x} are obtained as:

$$\begin{aligned}\frac{\partial\left(\varphi_{1x}(x_5, x_6)\right)}{\partial x_5} &= \frac{m}{u(t)}(\alpha_{1x}k_{1x} + 1),\\ \frac{\partial\left(\varphi_{1x}(x_5, x_6)\right)}{\partial x_6} &= \frac{m}{u(t)}(\alpha_{1x} + k_{1x}),\end{aligned}$$

$$\frac{\partial\left(V_{2x}\left(x_5,x_6\right)\right)}{\partial x_5}=\alpha_{2x}x_5\alpha_{1x}^2+\alpha_{2x}x_6\alpha_{1x}+x_5,$$
$$\frac{\partial\left(V_{2x}\left(x_5,x_6\right)\right)}{\partial x_6}=\alpha_{2x}x_6+\alpha_{1x}\alpha_{2x}x_5.$$

Considering expression (2), the virtual input u_{2x} is:

$$\begin{aligned}u_{2x}=&\frac{1}{m}\frac{u\left(\cdot\right)}{\cos(x_7)}\left(\alpha_{2x}x_6+\alpha_{1x}\alpha_{2x}x_5\right)-\frac{k_{2x}\sin(x_7)}{\cos(x_7)}\\&-\frac{k_{2x}m}{\cos(x_7)u\left(\cdot\right)}\left(x_5+\alpha_{1x}x_6+k_{1x}\left(x_6+\alpha_{1x}x_5\right)\right)\\&-\frac{1}{\cos(x_7)}\left(\sin(x_7)\right)\left(\alpha_1+k_{1x}\right)\\&+\frac{m}{u\left(\cdot\right)}\frac{x_6}{\cos(x_7)}\left(\alpha_{1x}k_{1x}+1\right).\end{aligned}$$

Finally, the last state variable is considered:

$$\begin{aligned}\dot{x}_5&=x_6\\\dot{x}_6&=-\tfrac{1}{m}\sin(x_7)u\left(\cdot\right)\\\dot{x}_7&=x_8\\\dot{x}_8&=\dot{\varphi}\dot{\psi}k_2+g_2\tau_\theta,\end{aligned}\tag{24}$$

and by the BS control algorithm the control τ_θ is obtained as:

$$\tau_\theta=\frac{1}{g_2}(-\dot{\varphi}\dot{\psi}k_2+\tau_{\theta a}).$$

Substituting the value of τ_θ in (24)

$$\begin{aligned}\dot{x}_5&=x_6\\\dot{x}_6&=-\frac{1}{m}\sin(x_7)u\left(\cdot\right)\\\dot{x}_7&=x_8\\\dot{x}_8&=\tau_{\theta a}.\end{aligned}$$

Similar to the previous subsystem, the last subsystem can be represented as:

$$\begin{bmatrix}\dot{x}_5\\\dot{x}_6\\\dot{x}_7\end{bmatrix}=\begin{bmatrix}x_6\\-u\left(\cdot\right)\sin(x_7)\\0\end{bmatrix}+\begin{bmatrix}0\\0\\1\end{bmatrix}\zeta_1$$
$$\dot{\zeta}_1=\tau_{\theta a},$$

where $\zeta_1=x_8$, and, the Lyapunov function V for this stage is proposed as:

$$\begin{aligned}&V_{3x}\left(x_5,x_6,x_7\right)\\&=\frac{1}{2}x_5^2+\frac{\alpha_{2x}}{2}\left(x_6+\alpha_{2x}x_5\right)^2\\&\quad+\frac{\alpha_{3x}}{2}\left(\sin(x_7)-\frac{m}{u\left(\cdot\right)}\left(x_5+\alpha_{1x}x_6+k_{1x}\left(x_6+\alpha_{1x}x_5\right)\right)\right)^2.\end{aligned}$$

The virtual input φ_{3x} is associated by u_{2x}

$$\begin{aligned}&\varphi_{3x}\left(x_5,x_6,x_7\right)\\&=\frac{1}{m}\frac{u\left(\cdot\right)}{\cos(x_7)}\left(\alpha_{2x}x_6+\alpha_{1x}\alpha_{2x}x_5\right)\\&\quad-\frac{k_{2x}}{\cos(x_7)}\left(\sin(x_7)-\frac{m}{u\left(\cdot\right)}\left(x_5+\alpha_{1x}x_6+k_{1x}(x_6+\alpha_{1x}x_5)\right)\right)\\&\quad-\frac{1}{\cos(x_7)}(\sin(x_7))(\alpha_{1x}+k_{1x})+\frac{m}{u\left(\cdot\right)}\frac{x_6}{\cos(x_7)}(\alpha_{1x}k_{1x}+1).\end{aligned}$$

Finally, the input $\tau_{\theta a}$ is

$$\begin{aligned}\tau_{\theta a}=&-k_{3x}\left(x_8-\varphi_{3x}\left(x_5,x_6,x_7\right)\right)\\&-\frac{\partial\left(V_{3x}\left(x_5,x_6,x_7\right)\right)}{\partial x_7}+x_6\frac{\partial\left(\varphi_{3x}\left(x_5,x_6,x_7\right)\right)}{\partial x_5}\\&-\left(\frac{u(\cdot)\sin(x_7)}{m}\right)\frac{\partial\left(\varphi_{3x}\left(x_5,x_6,x_7\right)\right)}{\partial x_6}\\&+x_8\frac{\partial\left(\varphi_{3x}\left(x_5,x_6,x_7\right)\right)}{\partial x_7}.\end{aligned}$$

In this way, the nonlinear control for the subsystem $x-\theta$ is calculated. In the next section, the controller synthesis for the subsystem $y-\varphi$ is presented.

D. SUBSYSTEM $y-\varphi$

Consider the subsystem $y-\varphi$, which describes the movement on the y axis and the roll angle, as follows:

$$\begin{aligned}\ddot{y}&=\frac{u}{m}\cos(\theta)\sin(\varphi)\\\ddot{\varphi}&=\dot{\theta}\dot{\psi}k_3+g_3\tau_\varphi,\end{aligned}$$

where $k_3=\frac{(\mathbb{I}_y-\mathbb{I}_z)}{\mathbb{I}_x}$ and $g_3=\frac{l}{\mathbb{I}_x}$, consider $x_9=y$, $x_{10}=\dot{y}$, $x_{11}=\varphi$, $x_{12}=\dot{\varphi}$. So, the state space representation is

$$\begin{aligned}\dot{x}_9&=x_{10}\\\dot{x}_{10}&=\frac{u\left(\cdot\right)}{m}\cos(x_7)\sin(x_{11})\\\dot{x}_{11}&=x_{12}\\\dot{x}_{12}&=\dot{\theta}\dot{\psi}k_3+g_3\tau_\varphi.\end{aligned}$$

For the first step, consider:

$$\begin{aligned}\dot{x}_9&=x_{10}\\\dot{x}_{10}&=\frac{u\left(\cdot\right)}{m}\cos(x_7)\sin(x_{11}),\end{aligned}\tag{25}$$

if the virtual input u_{1y} is selected as:

$$u_{1y}=\sin(x_{11})=\frac{m}{u\left(\cdot\right)\cos(x_7)}(u_{ay}),\tag{26}$$

by substituting the virtual control (26) into (25) it follows that:

$$\begin{aligned}\dot{x}_9&=x_{10}\\\dot{x}_{10}&=u_{ay}.\end{aligned}\tag{27}$$

Defining $x_{10}=\varphi(x_9)=-\alpha_{1y}x_9$, (27) can be rewritten as

$$\begin{aligned}\dot{x}_9&=\alpha_{1y}x_9\\\dot{x}_{10}&=u_{ay}.\end{aligned}$$

For the last dynamic, define a Lyapunov function as follows:

$$V_{1y}(x_9)=\frac{1}{2}x_9^2.\tag{28}$$

By using of the iterative BS algorithm, the input u_{ay} can be calculated as:

$$u_{ay}=-k_{1y}\left(x_{10}-\alpha_{3y}x_9\right)-x_9-\alpha_{3y}\left(x_{10}\right),\tag{29}$$

and substituting (29) into (26), the input u_{1y} is:

$$u_{1y}=\frac{m\left(-k_{1y}\left(x_{10}-\alpha_{1y}x_9\right)-x_9-\alpha_{1y}\left(x_{10}\right)\right)}{u\left(\cdot\right)\cos(x_7)}.$$

In the second step, the variable $\dot{x}_{11}$ is considered, and the state space is

$$\begin{aligned}\dot{x}_9 &= x_{10}\\ \dot{x}_{10} &= \frac{u(\cdot)}{m}\cos(x_7)\sin(x_{11})\\ \dot{x}_{11} &= x_{12},\end{aligned} \tag{30}$$

by using Proposition 1, system (30) can be rewritten as:

$$\begin{bmatrix}\dot{x}_9\\ \dot{x}_{10}\end{bmatrix} = \begin{bmatrix}x_{10}\\ 0\end{bmatrix} + \begin{bmatrix}0\\ \frac{u(\cdot)\cos(x_7)}{m}\end{bmatrix}\sin(\zeta_2)$$
$$\dot{\zeta}_2 = x_{12} = u_{2y},$$

where $\zeta_2 = x_{11}$. At this point, the augmented Lyapunov function is considered as:

$$V_{2y}(x_9, x_{10}) = \frac{1}{2}x_9^2 + \frac{\alpha_{2y}}{2}\left(x_{10} + \alpha_{1y}x_9\right)^2,$$

where α_{2y} is a positive constant. Now, the virtual input φ_{1y} is defined by:

$$\begin{aligned}u_{1y} &= \varphi_{1y}(x_9, x_{10})\\ &= \frac{m}{u(\cdot)\cos(x_7)}\left(-k_{1y}\left(x_{10} - \alpha_{1y}x_9\right) - x_9 - \alpha_{1y}(x_{10})\right),\end{aligned}$$

and by the iterative BS algorithm we obtain:

$$\begin{aligned}\frac{\partial(\varphi_{1x}(x_9, x_{10}))}{\partial x_9} &= \frac{m}{u(\cdot)\,cos(x_7)}(\alpha_{1y}k_{1y} + 1)\\ \frac{\partial\left(\varphi_{1y}(x_9, x_{10})\right)}{\partial x_6} &= \frac{m}{u(\cdot)}(\alpha_{1y} + k_{1y})\\ \frac{\partial\left(V_{2y}(x_9, x_{10})\right)}{\partial x_9} &= \alpha_{2y}x_5\alpha_{1y}^2 + \alpha_{2y}x_{10}\alpha_{1y} + x_9\\ \frac{\partial\left(V_{2y}(x_9, x_{10})\right)}{\partial x_{10}} &= \alpha_{2y}x_{10} + \alpha_{1y}\alpha_{2y}x_9.\end{aligned}$$

So, the new virtual input is:

$$\begin{aligned}u_{2y} = &\frac{1}{\cos(x_{11})}(\sin(x_{11}))\left(\alpha_{1y} + k_{1y}\right)\\ &+\frac{1}{m}u(\cdot)\frac{\cos(x_7)}{\cos(x_{11})}\left(\alpha_{2y}x_{10} + \alpha_{1y}\alpha_{2y}x_9\right)\\ &-\frac{mk_{2y}\left(x_9 + \alpha_{1y}x_{10} + k_{1y}\left(x_{10} + \alpha_{1y}x_9\right)\right)}{u(\cdot)\cos(x_{11})\cos(x_7)}\\ &-\frac{m}{u(\cdot)}\frac{x_{10}}{\cos(x_7)\cos(x_{11})}\left(\alpha_{1y}k_{1y} + 1\right) - \frac{k_{2y}\sin(x_{11})}{\cos(x_{11})}.\end{aligned}$$

For the last step, the dynamic of x_{12} is considered, so:

$$\begin{aligned}\dot{x}_9 &= x_{10}\\ \dot{x}_{10} &= \frac{u(\cdot)}{m}\cos(x_7)\sin(x_{11})\\ \dot{x}_{11} &= x_{12}\\ \dot{x}_{12} &= \dot{\theta}\dot{\psi}k_3 + g_3\tau_\varphi.\end{aligned} \tag{31}$$

Define the control action as:

$$\tau_\varphi = \frac{1}{g_3}(-\dot{\theta}\dot{\psi}k_2 + \tau_{\varphi a}). \tag{32}$$

Substituting (32) into the system given by (31) we get:

$$\begin{aligned}\dot{x}_9 &= x_{10}\\ \dot{x}_{10} &= \frac{u(\cdot)}{m}\cos(x_7)\sin(x_{11})\\ \dot{x}_{11} &= x_{12}\\ \dot{x}_{12} &= \tau_{\varphi a}.\end{aligned}$$

Considering the iterative BS algorithm, the previous subsystem is:

$$\begin{bmatrix}\dot{x}_9\\ \dot{x}_{10}\\ \dot{x}_{11}\end{bmatrix} = \begin{bmatrix}x_{10}\\ u(\cdot)\cos(x_7)\sin(x_{11})\\ 0\end{bmatrix} + \begin{bmatrix}0\\ 0\\ 1\end{bmatrix}\zeta_3$$
$$\dot{\zeta}_3 = \tau_{\varphi a},$$

where $\zeta_3 = x_{12}$. The Lyapunov function for this step, follows the value of V_{2y}

$$\begin{aligned}&V_{3y}(x_9, x_{10}, x_{11})\\ &= \frac{1}{2}x_9^2 + \frac{\alpha_{2y}}{2}\left(x_{10} + \alpha_{1y}x_9\right)^2\\ &\quad + \frac{\alpha_{3y}}{2}\left(\sin(x_{11}) + \frac{m\left(x_9 + \alpha_{1y}x_{10} + k_{1y}\left(x_{10} + \alpha_{1y}x_9\right)\right)}{u(\cdot)\cos(x_7)}\right)^2,\end{aligned}$$

and φ_{3y} is defined by

$$\begin{aligned}&\varphi_{3y}\\ &= \frac{(\sin(x_{11}))\left(\alpha_{1y} + k_{1y}\right)}{\cos(x_{11})} + \frac{u(\cdot)\cos(x_7)\left(\alpha_{5y}x_{10} + \alpha_{1y}\alpha_{2y}x_9\right)}{m\cos^2(x_{11})}\\ &\quad - \frac{k_{2y}\sin(x_{11})}{\cos(x_{11})} - \frac{k_{2y}m\left(x_9 + \alpha_{1y}x_{10} + k_{1y}\left(x_{10} + \alpha_{1y}x_9\right)\right)}{u(\cdot)\cos(x_7)\cos(x_{11})}\\ &\quad - \frac{m}{u(\cdot)}\frac{x_{10}}{\cos(x_7)\cos(x_{11})}\left(\alpha_{1y}k_{1y} + 1\right).\end{aligned}$$

Finally, the input $\tau_{\varphi a}$ is described as in (33).

$$\begin{aligned}\tau_{\varphi a} = &x_{10}\frac{\partial\left(\varphi_{3y}(x_9, x_{10}, x_{11})\right)}{\partial x_9}\\ &+\left(\frac{u(\cdot)}{m}\cos(x_7)\sin(x_7)\right)\frac{\partial\left(\varphi_{3y}(x_9, x_{10}, x_{11})\right)}{\partial x_{10}}\\ &+x_{12}\frac{\partial\left(\varphi_{3y}(x_9, x_{10}, x_{11})\right)}{\partial x_{11}} - \frac{\partial\left(V_{3y}(x_9, x_{10}, x_{11})\right)}{\partial x_{11}}\\ &-k_{3y}\left(x_{12} - \varphi_{3y}(x_9, x_{10}, x_{11})\right).\end{aligned} \tag{33}$$

These controllers are implemented in the experimental platform which is described in the following section.

E. EXPERIMENTAL PLATFORM

The aerial vehicle is built on a carbon fiber Frame of 550*mm*. A Pixhawk autopilot is mounted onboard. This autopilot has a high performance, its main clock runs at 168 MHz, and its processor is a 32 bit STM32F427 Cortex M4 core with FPU. It has two accelerometers, a gyroscope and two magnetometers which give accurate measurements of the vehicle attitude. A MEAS MS5611 barometer is added to estimate the altitude. Its weigh is just 38g and (50mm; 15.5mm; 81.5mm) for (H,W,L). It has RC signal input ports compatible with

FIGURE 1. Experimental platform used for test the proposed controller.

Futaba and Spektrum radios. Furthermore it has 8 PWM main outputs are used to control the motors. In order to know the longitudinal positions an external Ublox NEO-M8N GPS is installed which has an accuracy of 0.6m to 0.9m. This GPS has an internal magnetometer to estimate the yaw angle. The batteries used are LiPo technology, with a capacity of 4000 mA and a discharge rate C of 15. The vehicle has four 10 inches long propellers mounted and 4.5 propeller pitch. On the other hand, the desired trajectory was programmed into the autopilot by using a parametric circle equation, the parameter is the time t.

F. EXPERIMENTAL RESULTS USING THE BS AND SM CONTROL

In this subsection, experimental results of UAV flights are presented for both controllers, the modified BS and the SMC. In order to track a given trajectory in the translational space (x, y, z) and keep the rotational space (θ, φ, ψ) around the origin, the UAV flight task is given in three dimensional (x, y, z) space, and it is described in three paths: The first one is the takeoff in the time period $[0, 10)$ seconds. The trajectory is described by a straight line equation, where the references are $x_{ref} = 0, y_{ref} = 0$ and $z_{ref} = \frac{1}{2}t$. Notice that, the proposed control methods do not require the calculations of the wanted angles for a desired $x-y$ position, i.e. it obtains the necessary torques to be able to move the vehicle in a desired attitude (fixed to zero) and indirectly a desired position as well. Once the vehicle reaches the desired altitude, the second stage starts in the time period $[10, 58)$ seconds where the UAV tracks a trajectory given by a parametric circle equation. The system references for the second path are

$$\begin{aligned} x_{ref} &= -10\cos\left(\frac{\pi}{180}(t-10)\right)m \\ y_{ref} &= -10\sin\left(\frac{\pi}{180}(t-10)\right)m \\ z_{ref} &= 5m. \end{aligned} \tag{34}$$

Finally, in the time period $[58, 73)$ seconds a straight line equation with negative slope is designed for UAV landing. For this period the desired references is given by $x_{ref} = 0$, $y_{ref} = 0$, and $z_{ref} = \frac{1}{3}(73 - t)$. The sampling time (T) used in the flight test presented in this work, is $T = 0.01$ seconds. Moreover, for the desired altitude, a discretized straight line is used: $0.5\ t$, where $t = kT$ seconds, $k = 0, 1, 2, 3, ...$, and the performance of the take off task could be improved. The system parameters of this UAV are: Quad-rotor mass $m = 1.3\ kg$, the Inertia moments $\mathbb{I}_x = \mathbb{I}_y = 0.0023$ and $\mathbb{I}_z = 0.0054\ Kg \cdot m^2$. All the parameters of the plant were obtained by using the Solid Work software, introducing the frame characteristics into the software, and this gives an approximation of the plant parameters.

As mentioned earlier, a robust SMC algorithm was proposed to regulate the UAV altitude around the set-point. The set of parameters for the real time implementation of the SMC are $\rho = 18$, $R = 34$, $p = 1$ and $q = 3$. On the other hand, to improve the trajectory tracking behavior for subsystems ψ, $x - \theta$ and $y - \varphi$, the modified BS algorithm was designed in the present paper. Table 1, presents the modified BS control parameters introduced in the real time experiment. Actually, a PD controller is used to control the vehicle and its performance is compared to the proposed controllers. The PD controller is heuristically tuned by using the specifical time parameters overshot and settling time in closed loop, for details see [19].

Remark 1: Numerous tests were conducted using only the SMC and the BS algorithms (without the joint of both controllers) to regulate all the dynamics of the vehicle (these experimental results are omitted in this article because it was considered that they are not relevant to this contribution), however the combining of the SMC and modified BS controllers improve the performance of the closed loop system. The SMC applied to the x and y dynamics, the hardware (drivers and rotors) does not react with the necessary velocity to the control signal, which presents a relative high frequency compared to the hardware time response (490 Hz). The altitude control using SMC, gets better response, because the Set Point is fixed and the inertia moment $\mathbb{I}_z$ is greater than $\mathbb{I}_x$ and $\mathbb{I}_y$ inertia moments. Now, concerning the modified BS algorithm, the SMC approach applied to the altitude control allows to obtain control laws for the $x - \theta$ and $y - \varphi$ subsystems, relatively simpler, please notice that the control law for the altitude, appears as a disturbance on the $x - \theta$ and $y - \varphi$ subsystems, so we want to assure that the altitude control is bounded and converges in finite time. These characteristics are given by using the proposed SMC approach.

The gain ρ used in SMC, was characterized in such a way that this controller rejects external disturbances as air flow. This disturbance magnitude was heuristically estimated in the vehicle outdoor flight. In this way, one can guarantee that the altitude z will remain close to the desired set-point in finite time. Furthermore, trajectory ratio, in terms of its desired parametric equations (34), gives a circle with diameter of 20 meters. The initial conditions of the real time process, are around the origin of the system frame.

TABLE 1. Parameters for the aerial mission using the backstepping control.

ψ-subsystem	$x-\theta$ subsystem	$y-\varphi$ subsystem
$\alpha_\psi = 1.34$	$\alpha_{1x} = 1.57$	$\alpha_{1y} = 6.31$
$k_\psi = 67.2,$	$k_{1x} = 0.152$	$k_{1y} = 0.001$
	$\alpha_{2x} = 0.2$	$\alpha_{2y} = 0.19$
	$k_{2x} = 0.25$	$k_{2y} = 0.006$
	$\alpha_{3x} = 0.008$	$\alpha_{3y} = 0.001$
	$k_{3x} = 57.7$	$k_{3y} = 35.3$

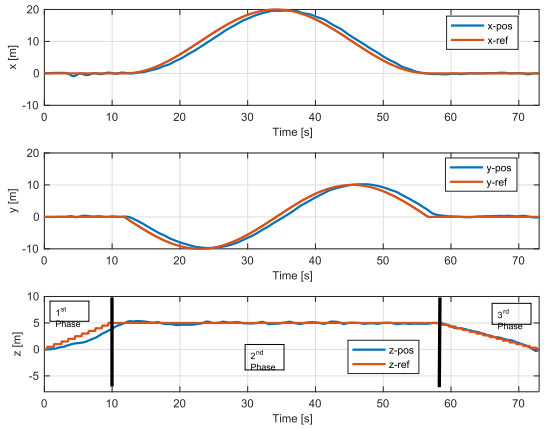

FIGURE 2. Position in the x, y and z axes applying the BS and SM controllers.

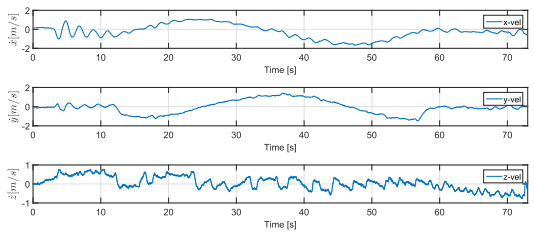

FIGURE 3. Velocities of the vehicle during the mission.

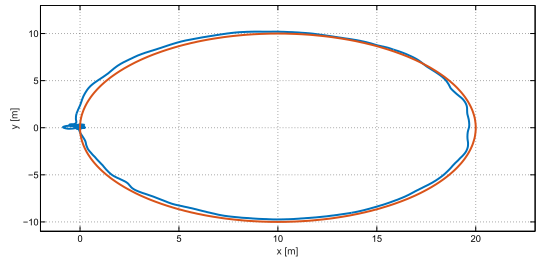

FIGURE 4. Trajectory x vs y during the task, applying a BS and SM controller.

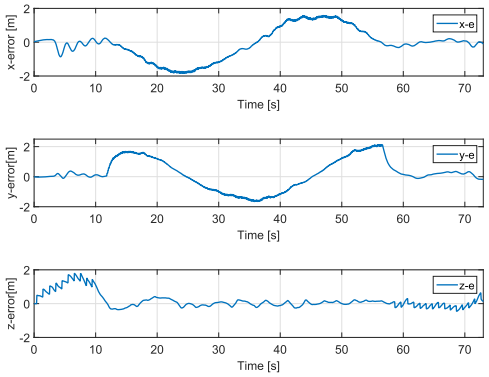

FIGURE 5. Signal of errors during the tracking of the trajectory.

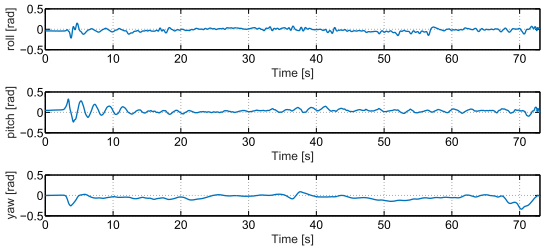

FIGURE 6. Attitude of the vehicle during the mission.

Figures 2-3, show the UAV translational positions and its velocities respectively. These figures are split into three subfigures: the first one depicts the trajectory performance along the X, the second one shows the system task in the Y. Finally, the UAV altitude performance is presented in the last subfigure. As depicted in Figure 2, where the system is in closed loop with the designed controllers, the translational positions in blue line have a good performance with respect to the desired values in red line. The deviation of the trajectory can be explained by the presence of external disturbances and the GPS devise accuracy.

The translational performance of the UAV, in the $X-Y$ space is shown in Figure 4. This figure shows how the system tracks the desired trajectory in task space.

Figure 5 shows the errors during the tracking of the trajectory. Notice that while the reference is changing in both axes, these errors may increase or decrease, but when the reference becomes constant these errors remain close to zero. Additionally, the measurements of the translational variables given by GPS, have a relative larger errors (from 0.6 m to 0.9 m) than the sensors used in the indoor environment (artificial vision for example); please notice that, the mean velocity of the vehicle, 3 km/h, and the cross wind presents along to the test, increase the tracking error. This explains the relative large error observed in the trajectory tracking displacement task.

Figure 6, depicts the vehicle's attitude. It is important here to notice that the Pitch, Yaw and Roll angles are around the UAV body frame.

Furthermore, the four control input signals in PWM (Pulse Width Modulation) percent, for altitude, pitch, yaw and roll respectively are presented in Figure 7. These control inputs are obtained with the modified BS and SMC algorithms and are applied in real experiments for tracking the desired trajectory. As can be seen from the figure, the maximum duty cycle is smaller than 40% and in some cases less than 20%, which represent less energy consumption and smoother control signals. This is an important issue when a nonlinear control is tuned in real time applications.

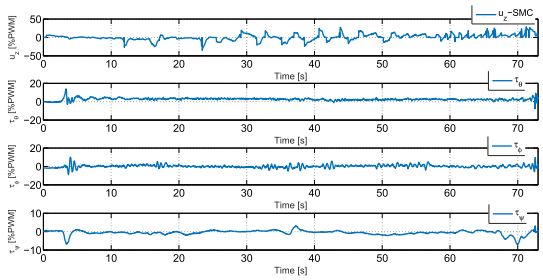

FIGURE 7. Control signals (BS and SM control).

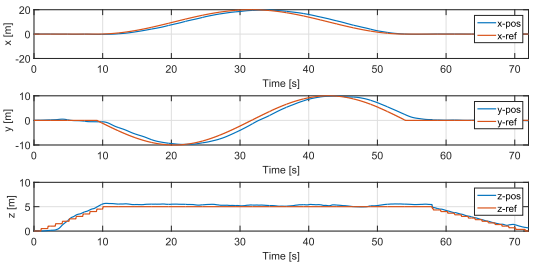

FIGURE 8. Position in the x, y and z axes applying a PD controller.

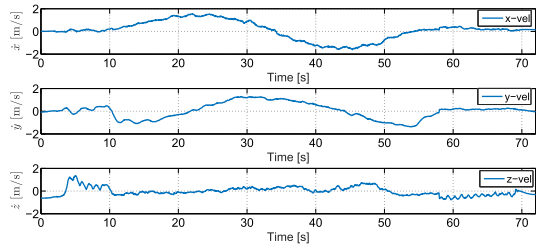

FIGURE 9. Velocities of the vehicle during the mission using a PD controller.

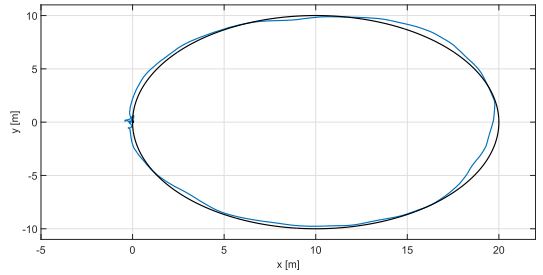

FIGURE 10. Trajectory x vs y during the task, applying a PD controller.

Figures 8-9, display the vehicle translational positions and its velocities respectively, for a PD control. This performance is compared to the proposed controllers by the calculation of the IAE performance index.

The translational performance in the $X-Y$ space of the UAV using a PD controller is shown in Figure 10.

Figure 11 shows the errors during the tracking of the trajectory when a PD controller is used. Figure 12, depicts the vehicle's attitude for a PD control.

The four control input signals in PWM (Pulse Width Modulation) percent, for altitude, pitch, yaw and roll respectively are presented in Figure 13.

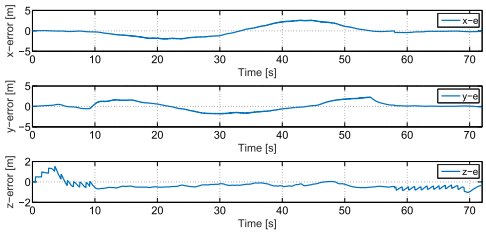

FIGURE 11. Signal of errors during the tracking of the trajectory when a PD controller is used.

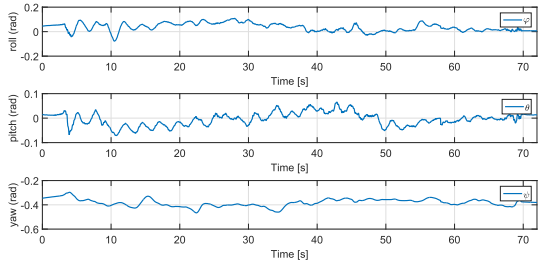

FIGURE 12. Attitude of the vehicle during the mission when a PD control is used.

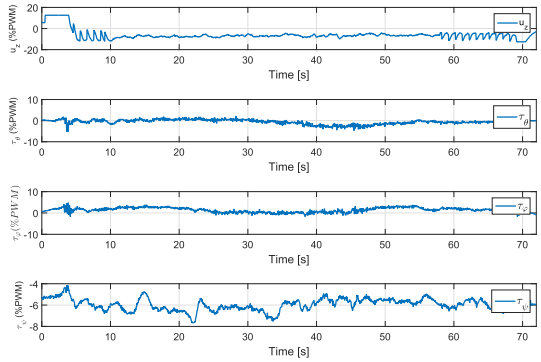

FIGURE 13. Control signals (PD control).

TABLE 2. Comparison of IAE during the aerial mission.

Indicator	*BS and SMC*	*PD*	σ_{BS-SMC}	σ_{PD}
IAE x	1351.63	1471.82	0.077	0.12
IAE y	1128.32	1289.06	0.07	0.12
IAE z	493.70	662.48	0.06	0.21

Finally, in order to demonstrate the effectiveness of the control and the repetitiveness of the experimental results, 10 tests were performed using the proposed modified BS, SMC and the PD controllers. These tests validated the experimental robustness of the proposed control laws in different outdoor scenarios with external disturbances. Furthermore, these results are summarized in Table 2, where the Integral Absolute Error (IAE) was obtained for each experiment, the standard deviation of the mean error was also added and it gives experimental evidence of the repetitiveness and reliability of our proposed control algorithms.

These tests also prove the feasibility of the proposed control algorithm. Actually, from this analysis, one concludes

that the system behavior of the proposed controller is very efficient. Also, according to the obtained experimental results, the BS and SMC have a better performance than the PD controller and more repeatability of the PD control.

V. CONCLUSIONS

Two control strategies were proposed to deal with the trajectory tracking problem of the quadrotor vehicle in outdoor environment. The altitude control is based on the SMC approach and guarantees the finite time convergence of the altitude and its velocity under the presence of bounded disturbances, in contrast to the PD controller which was tuned with the linear model. The finite time convergence of the state and the simplicity of the control law for the vehicle altitude allow the obtention of a simplified version of a modified BS control strategy for the translational and rotational variables, because the altitude control is a time function. Experimental results performed outdoors prove the feasibility, repetitiveness and reliability of the proposed control algorithms.

REFERENCES

[1] E. Altuğ, J. P. Ostrowski, and C. J. Taylor, "Control of a quadrotor helicopter using dual camera visual feedback," *Int. J. Robot. Res.*, vol. 24, no. 5, pp. 329–341, 2005.

[2] N. S. Özbek, M. Önkol, and M. Ö. Efe, "Feedback control strategies for quadrotor-type aerial robots: A survey," *Trans. Inst. Meas. Control*, vol. 38, no. 5, pp. 529–554, 2016.

[3] C. K. Tan, J. Wang, Y. C. Paw, and T. Y. Ng, "Tracking of a moving ground target by a quadrotor using a backstepping approach based on a full state cascaded dynamics," *Appl. Soft Comput.*, vol. 47, pp. 47–62, Oct. 2016.

[4] D. Cabecinhas, R. Cunha, and C. Silvestre, "A nonlinear quadrotor trajectory tracking controller with disturbance rejection," *Control Eng. Pract.*, vol. 26, pp. 1–10, May 2014.

[5] C. Li, Y. Zhang, and P. Li, "Full control of a quadrotor using parameter-scheduled backstepping method: Implementation and experimental tests," *Nonlinear Dyn.*, vol. 89, no. 2, pp. 1259–1278, 2017.

[6] J. J. Xiong and E.-H. Zheng, "Position and attitude tracking control for a quadrotor UAV," *ISA Trans.*, vol. 53, no. 3, pp. 725–731, 2014.

[7] Z. Zuo, "Non-singular fixed-time terminal sliding mode control of non-linear systems," *IET Control Theory Appl.*, vol. 9, no. 4, pp. 545–552, Feb. 2015.

[8] D. Lee, H. J. Kim, and S. Sastry, "Feedback linearization vs. Adaptive sliding mode control for a quadrotor helicopter," *Int. J. Control, Automat. Syst.*, vol. 7, no. 3, pp. 419–428, 2009.

[9] A. Kacimi, A. Mokhtari, and B. Kouadri, "Sliding mode control based on adaptive backstepping approch for a quadrotor unmanned aerial vehicle," *Przeglad Elektrotechniczny*, vol. 88, no. 6, pp. 188–193, 2012.

[10] B. Zhao, B. Xian, Y. Zhang, and X. Zhang, "Nonlinear robust adaptive tracking control of a quadrotor UAV via immersion and invariance methodology," *IEEE Trans. Ind. Electron.*, vol. 62, no. 5, pp. 2891–2902, May 2015.

[11] Y. Shtessel, C. Edwards, L. Fridman, and A. Levant, *Sliding Mode Control and Observation*, vol. 10. New York, NY, USA: Birkhäuser, 2014, p. 978.

[12] S. Bouabdallah and R. Siegwart, "Backstepping and sliding-mode techniques applied to an indoor micro quadrotor," in *Proc. IEEE Int. Conf. Robot. Automat. (ICRA)*, Apr. 2005, pp. 2247–2252.

[13] J.-J. Xiong and G.-B. Zhang, "Global fast dynamic terminal sliding mode control for a quadrotor UAV," *ISA Trans.*, vol. 66, pp. 233–240, Jan. 2017.

[14] Y. Feng, X. Yu, and Z. Man, "Non-singular terminal sliding mode control of rigid manipulators," *Automatica*, vol. 38, no. 12, pp. 2159–2167, 2002.

[15] M. Zhihong and X. H. Yu, "Terminal sliding mode control of MIMO linear systems," *IEEE Trans. Circuits Syst. I, Fundam. Theory Appl.*, vol. 44, no. 11, pp. 1065–1070, Nov. 1997.

[16] A. Aboudonia, A. El-Badawy, and R. Rashad, "Active anti-disturbance control of a quadrotor unmanned aerial vehicle using the command-filtering backstepping approach," *Nonlinear Dyn.*, vol. 90, no. 1, pp. 581–597, 2017.

[17] Z. Zuo, "Trajectory tracking control design with command-filtered compensation for a quadrotor," *IET Control Theory Appl.*, vol. 4, no. 11, pp. 2343–2355, Nov. 2010.

[18] D. E. Kirk, *Optimal Control Theory: An Introduction*. Chelmsford, MA, USA: Courier Corporation, 2012.

[19] O. Santos, H. Romero, S. Salazar, O. García-Pérez, and R. Lozano "Optimized discrete control law for quadrotor stabilization: Experimental results," *J. Intell. Robotic Syst.*, vol. 84, nos. 1–4, pp. 67–81, 2016.

[20] J. Hauser, S. Sastry, and G. Meyer, "Nonlinear control design for slightly non-minimum phase systems: Application to V/STOL aircraft," *Automatica*, vol. 28, no. 4, pp. 665–679, 1992.

[21] H. K. Khalil, *Nonlinear Systems*, vol. 2. Upper Saddle River, NJ, USA: Prentice-Hall, 1996, pp. 1–5.

[22] M. A. M. Basri, A. R. Husain, and K. A. Danapalasingam, "Stabilization and trajectory tracking control for underactuated quadrotor helicopter subject to wind-gust disturbance," *Sadhana*, vol. 40, no. 5, pp. 1531–1553, 2015.

[23] M. R. Mokhtari and B. Cherki, "A new robust control for minirotorcraft unmanned aerial vehicles," *ISA Trans.*, vol. 56, pp. 86–101, May 2015.

[24] R. Bitmead, "Persistence of excitation conditions and the convergence of adaptive schemes," *IEEE Trans. Inf. Theory*, vol. 30, no. 2, pp. 183–191, Mar. 1984.

[25] R. T. Y. Thien and Y. Kim, "Decentralized formation flight via PID and integral sliding mode control," *Aerosp. Sci. Technol.*, vol. 81, pp. 322–332, Oct. 2018.

[26] S. Bouabdallah and R. Siegwart, "Full control of a quadrotor," in *Proc. IEEE/RSJ Int. Conf. Intell. Robots Syst.*, Oct./Nov. 2007, pp. 153–158.

[27] R. Lozano, *Unmanned Aerial Vehicles: Embedded Control*. Hoboken, NJ, USA: Wiley, 2013.

[28] V. K. Tripathi, L. Behera, and N. Verma, "Design of sliding mode and backstepping controllers for a quadcopter," in *Proc. 39th Nat. Syst. Conf. (NSC)*, Dec. 2015, pp. 1–6.

ORLANDO GARCÍA was born in Veracruz, Mexico, in 1988. He received the bachelor's degree in computer systems engineering from the Technological Institute of Poza Rica, in 2011, and the M.S. degree in autonomous systems of underwater and aerial navigation from UMI-CNRS, CINVESTAV-IPN, in 2015, where he is currently pursuing the Ph.D. degree. His thesis is on optimal trajectories in a quadcopter. His research interests include unmanned aerial vehicles (UAV's), real-time applications, embedded systems, and optimal control.

PATRICIO ORDAZ received the bachelor's degree in electronic and telecommunications engineering and the M.Sc. degree in automatic control from the Autonomous University of Hidalgo State, Hidalgo, Mexico, in 2004 and 2007, respectively, and the Ph.D. degree in automatic control from CINVESTAV, Mexico City, in 2012. He is currently with the Autonomous University of Hidalgo State. His research interests include the nonlinear control systems, robust control, adaptive control, system identification, and observation.

OMAR-JACOBO SANTOS-SÁNCHEZ received the B.S. degree from the Minatitlán Institute of Technology, Minatitlán, Mexico, and the M.S. degree in electrical engineering with option on automatic control and the Ph.D. degree from the Department of Automatic Control, CINVESTAV-IPN, Mexico, in 2000 and 2006, respectively. Since 2001, he has been with the State Autonomous University of Hidalgo, Pachuca, Mexico. His research interests include time-delay systems, and optimal and nonlinear control.

SERGIO SALAZAR was born in Tlaxcala, Mexico, in 1966. He received the B.S. degree in electronics engineering from the Benemérita Universidad Autónoma de Puebla, Puebla, Mexico, in 1992, the M.Sc. degree in electrical engineering from the Centro de Investigación y de Estudios Avanzados, Mexico City, Mexico, in 1995, and the Ph.D. degree in automatic control from the University of Technology of Compiègne (UTC), Compiègne, France, in 2005. Since 2008, he has been with the Laboratorio Franco-Mexicano de Informática y Automática Aplicada, Franco-Mexicano de Informática y Automática Aplicadas, Centre National de la Recherche Scientific, Centro de Investigación y de Estudios Avanzados. His current research interests include real-time control applications, embedded systems, unmanned aerial vehicles, and nonlinear dynamics and control.

ROGELIO LOZANO was born in Monterrey, Mexico, in 1954. He received the B.S. degree in electronic engineering from the National Polytechnic Institute, Mexico City, Mexico, in 1975, the M.S. degree in electrical engineering from the Centro de Investigación y de Estudios Avanzados (CINVESTAV), Mexico City, in 1977, and the Ph.D. degree in automatic control from the Laboratoire d'Automatique de Grenoble, Grenoble, France, in 1981. From 1981 to 1989, he was with the Department of Electrical Engineering, CINVESTAV, where he was the Head of the Section of Automatic Control, from 1985 to 1987. He held visiting positions at The University of Newcastle, Australia, from 1983 to 1984, the NASA Langley Research Center, Langley, VA, USA, from 1987 to 1988, and the Laboratoire d'Automatique de Grenoble, from 1989 to 1990. He was promoted to first-class CNRS Research Director, in 1997. From 1995 to 2007, he was the Head of the Laboratory Heudiasyc, UMR 6599, CNRS-University of Technology of Compiègne (UTC), Compiègne, France. Since 1990, he has been the CNRS Research Director of UTC. He is currently the Head of the Laboratorio Franco-Mexicano de Informática y Automática Aplicada, UMI-CNRS, CINVESTAV. His current research interests include adaptive control of linear and nonlinear systems, robot manipulators, passive systems, teleoperation, and unmanned aerial vehicles. From 1987 to 2000, he was an Associate Editor of *Automatica*. He has been an Associate Editor of the *International Journal of Adaptive Control and Signal Processing*, since 1993.